SECOND EUROPEAN CONFERENCE ON EARTHQUAKE ENGINEERING AND SEISMOLOGY, ISTANBUL AUG. 25-29, 2014

# PARAMETRIC STUDY OF THE POUNDING EFFECT BETWEEN ADJACENT RC BUILDINGS WITH ALIGNED SLABS

Francisco LÓPEZ-ALMANSA[1] and Alireza KHARAZIAN[2]

## ABSTRACT

This paper describes the initial steps of a parametrical numerical study about the consequences of pounding between adjoining short-to-mid height RC framed buildings with aligned slabs. Two 3 and 5-storey buildings are selected to represent the most common situations. The buildings are designed for a high seismicity region; their structure consists of square columns, rectangular deep beams and flat slabs. The study consists of analysing the dynamic response of the colliding buildings to a number of representative strong seismic inputs. Pounding is described by a Kelvin-Voight linear gap model. The nonlinear behaviour of the buildings structure is simulated with frame finite element models; nonlinearities are concentrated in plastic hinges whose moment-curvature is depicted by fibre models. Preliminary results show regular and expected results, this corroborating the accuracy and reliability of the considered model.

## INTRODUCTION

Pounding between adjoining buildings during strong seismic events is very common, despite the restraining recommendations of the design codes. Pounding significantly modifies the dynamic behaviour during input ground motions, both in terms of relative displacements and of absolute accelerations; therefore, it must be considered for a proper evaluation of the seismic performance. The worst case corresponds to unaligned slabs (floor-to-column pounding) since the impact of massive and rigid slabs against the mid-height of columns can break them and then lead to overall structural collapse; however, the collision between aligned slabs (floor-to-floor pounding) is more common and can be also highly threatening. This paper focusses in pounding between RC (reinforced concrete) buildings with aligned slabs.

Since pounding is highly relevant for seismic design and analysis, a number of researches have been reported; given that the accurate modelling of pounding is rather difficult, most of the studies deal mainly with such issue.

- **Anagnostopoulos 1988**. A simplified model for the pounding amongst several adjacent buildings is used. It is shown that the end structures experience almost always substantial increases in their response while for ‘interior’ structures the opposite often happens.
- **Maison, Kasai 1992**. A formulation and solution of the multiple-degree-of-freedom equations of motion for floor-to-floor pounding between two 15-storey and 8-storey buildings are presented. The influence of building separation, relative mass, and contact location properties are assessed.
- **Papadrakakis et al. 1996**. A three-dimensional model is developed for the simulation of the pounding response of two or more adjacent buildings. With this three-dimensional idealization, the effect of various in-plan configurations of adjacent buildings as well as the induced deformations

[1] Professor, Technical University of Catalonia, Barcelona, francesc.lopez-almansa@upc.edu
[2] PhD Student, Technical University of Catalonia, Barcelona, alireza.kharazian@estudiant.upc.edu

due to torsion during pounding are investigated for two real earthquake motions. The combination of flexible and stiff adjacent buildings results in an amplification effect during pounding on the stiff structure, particularly when the excitation is near the resonance of the flexible building, and in a mitigation effect on the flexible building.

- **Pantelides, Ma 1998**. The structural response of SDOF models with either elastic or inelastic structural behaviour is analysed. The pounding phenomenon is modelled as a Hertz impact force. Numerical simulations have shown that the pounding response is not highly sensitive to the impact stiffness parameter. For colliding structures with different natural periods, the same earthquake excitation can produce different magnitudes of pounding force and resulting structural response.
- **Ruangrassamee, Kawashima 2001**. This paper deals with bridges. This research investigates the effect of pounding on the relative displacement between two adjacent bridge segments. The energy lost in pounding is neglected. The results are represented in the form of normalized relative displacement response spectra with pounding effect. It is found that pounding can amplify the relative displacement.
- **Chau, Wei 2001**. A new non-linear Hertzian formulation is proposed to model pounding between two adjacent structures with different natural periods and damping ratios, under harmonic excitation. The impact velocity increases drastically when the difference in natural periods between the two structures increases. The impact velocity is relatively insensitive to the gap size. The maximum relative impact velocity can occur at an excitation period which is either between those of the two oscillators or less than both of them. Parametric studies show that the maximum relative impact velocity is not very sensitive to changes in the contact parameters.
- **Anagnostopoulos 2004**. In studies of earthquake-induced pounding between adjacent structures, spring–dashpot elements are often used to simulate the impacts. In this paper an equation expressing the dashpot constant as a function of the coefficient of restitution is derived.
- **Karayannis, Favvata 2005**. This paper deals both with aligned and unaligned slabs; only the first case is described here. The columns ductility requirements were bigger where the gap is smaller. The ductility requirements of the columns of the taller building are substantially increased for the floors above the contact level probably due to a whiplash behaviour.
- **Jankowski 2005**. This paper aims to analyse a non-linear viscoelastic model of collisions. The effectiveness of the model is verified by comparing the results of numerical analyses with the results of experiments conducted on pounding between different types of structures. The proposed non-linear viscoelastic model is the most precise one in simulating the pounding-involved structural response.
- **Jankowski 2006a**. This paper proposes the idea of impact force response spectrum for two structures; peak pounding force vs. natural periods. Pounding has been simulated by nonlinear viscoelastic model. The structural parameters, such as gap, natural periods, damping, mass and ductility as well as the time lag of input ground motion records, might have a substantial influence.
- **Jankowski 2006b**. It has been verified that the non-linear viscoelastic model may be considered most accurate. The aim of this paper is to derive an approximating formula relating the impact damping ratio with the coefficient of restitution.
- **Muthukumar, DesRoches 2006**. This paper investigates the capacity of various impact models to reproduce the seismic pounding response. The considered models are: linear spring, linear Kelvin and Hertz models, and non-linear hysteresis damper (Hertz damp model). Simple analytical approaches to estimate the impact stiffness parameters of these models are proposed. The linear Hertz model provides adequate results at low PGA levels, and the Hertz damp model is recommended at moderate and high PGA levels.
- **Jankowski 2008**. This paper presents a detailed investigation on pounding-involved response of two equal-height buildings with substantially different dynamic properties. Results show that collisions have a significant influence on the lighter and more flexible building, whereas the response of the heavier and stiffer structure can be influenced only negligibly.
- **Dimitrakopoulos, Kappos, Makris 2009a**. The dynamic response of two and three pounding oscillators subjected to pulse-type excitations is revisited with dimensional analysis. It is shown that regardless of the acceleration level and duration of the pulse all response spectra become self-similar and follow a single master curve. This is true despite the realization of finite duration contacts with increasing durations as the excitation level increases. All physically realizable contacts (impacts,

continuous contacts, and detachments) are captured via a linear complementarity approach. The study confirms the existence of three spectral regions. The response of the most flexible among the two oscillators amplifies in the low range of the frequency spectrum (flexible structures); whereas, the response of the most stiff among the two oscillators amplifies at the upper range of the frequency spectrum (stiff structures). Most importantly, the study shows that pounding structures such as colliding buildings or interacting bridge segments may be most vulnerable for excitations with frequencies very different from their natural eigen-frequencies. Finally, by applying the concept of intermediate asymptotics, the study unveils that the dimensionless response of two pounding oscillators follows a scaling law with respect to the mass ratio, or in mathematical terms, that the response exhibits an incomplete self-similarity or self-similarity of the second kind with respect to the mass ratio.

- **Dimitrakopoulos, Kappos, Makris 2009b**. Starting from the previous work of the authors which focused on pulse-type excitations, the paper deals with arbitrary excitations. The study proposes input selection criteria and shows that the proposed approach reduces drastically the scatter in the response.
- **Ye, Li, Zhu 2009**. In this paper, re-examination of the Hertz contact model with nonlinear damping is made. The formula used to determine the damping constant in terms of the spring stiffness, the coefficient of restitution and relative approaching velocity of two colliding bodies is found to be incorrect for pounding simulation. A more accurate approximating formula for the damping constant is derived.
- **Jankowski 2010**. This paper describes two experiments. The first experiment consisted in dropping balls onto a rigid surface, whereas the second one focused on pounding-involved response of two tower models on a shaking table. The results of the shaking table tests show a considerable influence of the material of the colliding elements on the seismic behaviour of the tested models.
- **Cole et al. 2010**. This paper aims to assist engineers undertaking either preliminary or in-depth assessment of buildings with pounding potential. Floor-to-floor collisions are identified as a fundamentally different process to floor-to-column collisions. Current methods of building pounding assessment are reviewed. Critical building weaknesses vulnerable to pounding are presented.
- **Raj et al. 2010**. In this paper, simulation of seismic pounding between 8-story and 10-story framed RC buildings is presented. Modified Kelvin-Voigt (MKV) model and modified Kelvin (MK) model are compared; the MKV model is more rational than the MK model. The response of the 8-story building is amplified due to pounding. The pounding response is found to be more dependent on earthquake characteristics than on the gap between buildings.
- **Boyer et al. 2012**. A linear and non-linear model are developed to analyse the structural impact of two single-degree-of-freedom structures. Different impact coefficients of restitution, normalized distances between structures and structural periods are considered.
- **Favvata et al. 2012**. The pounding between adjacent RC structures with unequal heights is investigated taking into account the infills. Solid masonry infills and infills with openings panels are considered.
- **Yaghmaei-Sabegh, Jalali-Milani 2012**. As a practical tool, the pounding force response spectrum, which shows the value of maximum impact force as a function of the structural vibration periods, is considered. Pounding force response spectra for elastic structures subjected to near-field and far-field ground motions are presented. The effect of mass, gap distance and damping ratio has been studied; in contrast to common acceptance that the pounding force decreases with gap distance increasing, some exceptions have been shown.
- **Barros et al. 2013**. Two RC models are considered to compare the effectiveness of Base Isolation against fixed support. The results of different link elements are compared.
- **Efraimiadou et al. 2013**. The effect of different structural configurations on the collision between adjacent planar RC 5-storey and two 8-storey building frames is examined. The effect of collision of adjacent frames seems to be unfavourable for most of the cases.
- **Khatiwada et al. 2014**. Most of contact models are based on the collision of idealized concentrated masses, while the pounding structures have distributed masses. These models also have uncertainties regarding the stiffness of the links, the lost energy and the contact duration. Other pounding models are based in stress wave propagation. This paper proposes a quasi-empirical impact mechanism for

simulation of structural pounding. The model includes the effects of the contact surface and cross-sectional properties.

Despite this extensive previous research, there are still many open questions; among them, perhaps the most relevant is the lack of a comprehensive study about the practical consequences of pounding between adjoining buildings. The objective of this research is to contribute to close this gap by investigating the major consequences of pounding between adjacent buildings with aligned slabs (floor-to-floor impact). The study focusses in the most common and relevant cases, namely symmetric short-to-mid height RC buildings located in high seismicity regions and undergoing severe ground motions. A number of buildings and seismic registers are selected to represent the most frequent and relevant situations. The pounding is simulated by nonlinear dynamic analyses of the colliding buildings under the considered inputs. The pounding effect is described with linear Kelvin-Voight (spring-dashpot) gap models located in each storey. The nonlinear dynamic structural behaviour of the frames is described with frame finite element models where nonlinearities are concentrated in plastic hinges depicted by fibre models. The pounding relevance is quantified in terms of the following response magnitudes: maximum and cumulated inter-storey drift, maximum absolute acceleration, and maximum base shear; these magnitudes report about the structural damage, the non-structural damage and the demand on the foundation, respectively.

The final objective of this research is to propose simplified criteria for describing the pounding effects; these criteria might be incorporated into the design codes.

## REPRESENTATIVE PROTOTYPE BUILDINGS

Two housing or administrative prototype buildings have been selected to represent the most common situations. Both buildings have RC structure with square columns, two-way solid slabs and rectangular cast-in-situ beams joining the columns, see Figure 1.

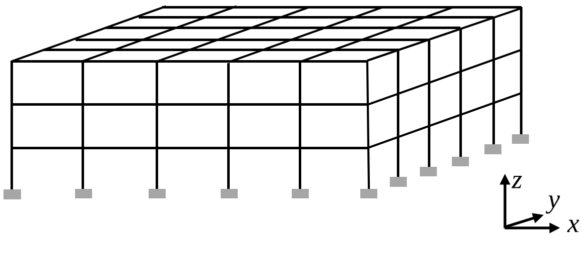


(a) Three-story building

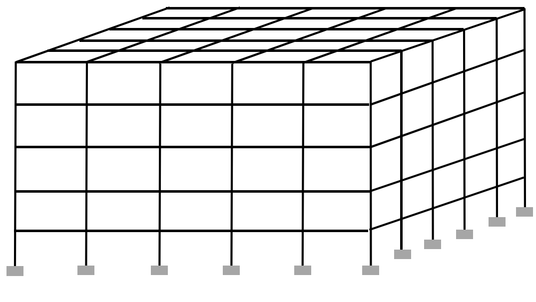

(b) Five-story building

**Figure 1.** Pounding buildings

As shown in Figure 1, both buildings have uniformity in elevation and plan symmetry, with rectangular plan layout with six frames (five bays) in direction parallel to the joint between the buildings (*y*); in the other direction (*x*) the number of bays of each building ranges in between two and five to account for the differences in mass among both buildings. One of the buildings is 3-storey (Figure 1.a) while the other one is 5-storey (Figure 1.b). The storey height is 3.2 m and the span length is 5 m in both directions. The beams section is 40 × 50 cm$^2$ and the slabs are 15 cm deep. Inside each storey all the columns are alike, even the reinforcement; Table 1 depicts the cross sections of the columns. The characteristic values of the concrete compressive strength and of the steel yielding point are $f'_c$ = 30 MPa and $f_y$ = 400 MPa, respectively. The buildings are designed according to the ACI and ASCE codes (ACI-318 2011, ASCE/SEI 7-10 2010). Dead loads: self-weight + flooring + partitioning = 8 kN/m$^2$, roof self-weight + flooring + partitioning = 6.8 kN/m$^2$, cladding 3/2.6 kN/m$^2$. Live loads: floors 2 kN/m$^2$, roof 1.5 kN/m$^2$, stairs 3.5 kN/m$^2$. The loading combination is 1.2 $D$ + 1.2 $L$. The seismic design is performed for 0.4 g design acceleration, corresponding to 475 years return period (10% probability of being exceeded in 50 years). The soil is stiff, with shear wave velocity in between 180 and 360 m/s; it corresponds to type D according to the ASCE classification (ASCE/SEI 7-10 2010) and to type C according to the EC-8 classification (EN-1998 2004). For design purposes, the structure of the buildings is modelled as a 3D frame of beams and columns with rigid connections among them; the columns are assumed to be clamped to the foundation. The beams are modelled as T-section members; the effective width is 105 cm for the inner beams and 70 cm for the side beams (ACI-318 2011). The concrete cracking is taken into account by reducing the moments of inertia of beams and columns by factors 0.35 and 0.7, respectively. The contribution of the staircases, infill walls and other elements to the lateral resistance of the building is neglected. The seismic design is carried out through equivalent static analysis. For serviceability conditions, the drift limit is 0.02 $H$ for the 3-storey building and 0.025 $H$ for the 5-storey building. The fundamental periods of the buildings are estimated from the empirical expressions contained in the ASCE code; for the 3 and 5-storey buildings it is initially assumed that $T_F$ = 0.3 s and 0.5 s, respectively. The assumed damping factor is 5%. The buildings are considered of normal importance and the response reduction factor is 5, corresponding to "intermediate reinforced concrete moment frames" according to the ASCE code. The contributing mass of the slab is uniformly distributed among all the frames. The site seismicity for 4975 years return period (1% probability of being exceeded in 50 years) corresponds to coefficients $S_S$ = 2.098 g, $S_1$ = 0.994 g (spectral response acceleration parameters), $F_a$ = 1, $F_v$ = 1.5 (site coefficients based on and $S_S$ and on $S_1$, respectively); in the design spectrum the left and right abscissae of the plateau are $T_0$ = 0.142 s and $T_S$ = 0.711 s, respectively.

**Table 1**. Column dimensions (cm × cm)

| **5-storey building. Floor No.** | | | | | **3-storey building. Floor No.** | | |
|---|---|---|---|---|---|---|---|
| 1 | 2 | 3 | 4 | 5 | 1 | 2 | 3 |
| 60 × 60 | 55 × 55 | 50 × 50 | 45 × 45 | 40 × 40 | 50 × 50 | 45 × 45 | 40 × 40 |

In the designed buildings, the diameter of the longitudinal reinforcement bars ranges in between 20 and 25 mm while the diameter of the transverse reinforcement is 10 mm. The fundamental periods corresponding to $D$ + 0.2 $L$ are $T_F$ = 0.382 s for the 3-storey building and $T_F$ = 0.524 s for the 5-storey building. Comparison with the originally estimated values (previous paragraph) shows that the frames are slightly more flexible than expected; the equivalent static forces are not recomputed since the difference is small.

## POUNDING DESCRIPTION

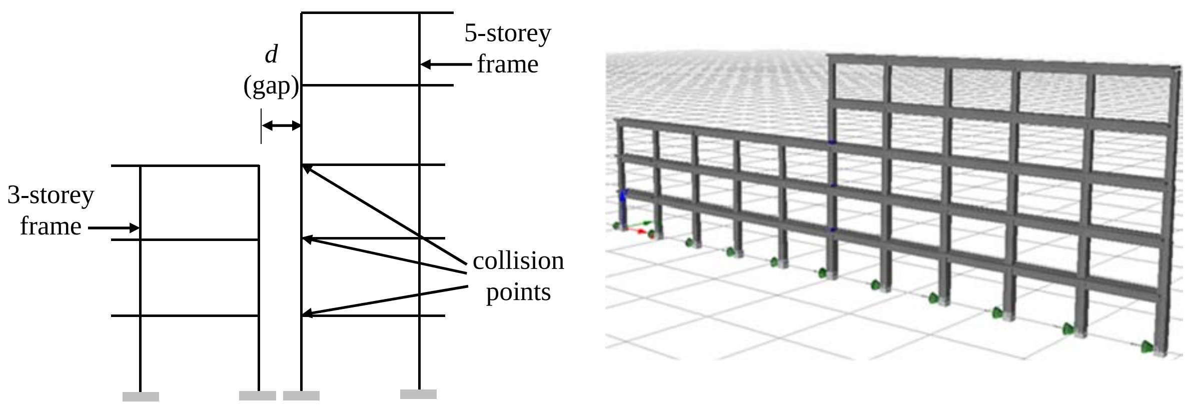


(a) Sketch of the frames (b) Numerical model of the frames

**Figure 2**. Considered pounding frames

The prototype buildings described in the previous section are assumed to collide by pairs; moreover, the 5-storey building without the two top floors is also contemplated. Along this study, $N$ represents the number of storeys and $b$ is the number of bays in direction orthogonal to the joint between the buildings ($x$, Figure 1); every building is denoted by $N \times b$. The 5-storey buildings without the two top floors are named by $(5 - 2) \times b$. As an example, Figure 2 describes pounding between $3 \times 5$ and $5 \times 5$ buildings .Figure 2.a shows a detail of two colliding frames and Figure 2.b displays a 3D global representation of such frames; this last image has been taken from the numerical model considered in the analysis. The gap indicated in Figure 2.a represents the initial separation between the frames; the considered values of the gap size ($d$) are 0.5, 1, 2 and 3 cm. Noticeably, for 4 cm there is no pounding in virtually all the situations.

The pounding effect is described with linear Kelvin-Voight gap models (parallel combination of a spring and a dashpot) located in each storey. The stiffness ($k$) of the spring is selected proportional to the axial stiffness of the colliding slabs as $k = \alpha\ (E\ A\ /\ L)$ where $\alpha$ is a coefficient ($\alpha > 1$) and $E$, $A$ and $L$ are the modulus of elasticity (concrete), cross-section area and length of the longest colliding slab (Muthukumar, DesRoches 2006). Coefficient $\alpha$ accounts for the higher influence of the slab segments that are closer to the impact point. The damping coefficient is chosen as to provide a desired restitution factor ($r$) as $\zeta = -\ln r\ /\ (\pi^2 + \ln^2 r)^{1/2}$ (Anagnostopoulos 2004). Three values of the restitution factor are considered: 1, 0.6 and 0.5; the corresponding values of the damping factor are 0, 0.16 and 0.22, respectively.

## NUMERICAL MODELING OF THE STRUCTURAL BEHAVIOR

The nonlinear dynamic structural behaviour of the frames is described with frame finite element models (Figure 2.b); nonlinearities are concentrated in plastic hinges whose moment-curvature performance is depicted by fibre models SeismoStruct (Seismosoft 2013) with 150 fibres in each transversal section. The nonlinear behaviour of the concrete is represented by a five-parameter constant-confinement concrete model (Mander, Priestley, Park, 1988; Martínez-Rueda, Elnashai, 1997; Madas, 1993); the confinement effect is described by an effective confinement stress which depends on the longitudinal and transverse reinforcement. Since this model can experience numerical instabilities under large displacements, the modifications suggested by (Martínez-Rueda, Elnashai, 1997) are considered; the therefrom-arising model can predict the strength and stiffness degradation under cyclic motion. The behaviour of the reinforcement steel is described by uniaxial bilinear constitutive laws with 5‰ kinematic strain hardening; the hardening rule for the yield surface is a linear function of the increment of plastic strain. The diaphragm effect of the floor slabs is taken into account by imposing rigid constraints among all the joints belonging to the same slab.

The fundamental periods are obtained by classic linear eigenvalue analysis. Table 2 displays the computed fundamental periods of the individual and coupled buildings; in Table 2, “coupled buildings” refer to the joint behaviour of a pair of buildings moving together during their contact.

**Table 2**. Fundamental periods (s) of the individual and coupled buildings

| Building | | | | | | Pairs of buildings | | | | |
|---|---|---|---|---|---|---|---|---|---|---|
| 3 × 5 | 3 × 2 | 5 × 5 | (5 – 2) × 5 | (5 – 2) × 3 | (5 – 2) × 2 | 3 × 5 \| 5 × 5 | 3 × 2 \| 5 × 5 | 3 × 5 \| (5 – 2) × 5 | 3 × 5 \| (5 – 2) × 3 | 3 × 5 \| (5 – 2) × 2 |
| 0.382 | 0.357 | 0.524 | 0.293 | 0.287 | 0.280 | 0.484 | 0.497 | 0.327 | 0.334 | 0.339 |

Most of the omitted coupled buildings in Table 2 (e.g. $3 \times b \mid 3 \times b$, $5 \times b\ \mid 5 \times b$) correspond to two alike buildings, without relevant pounding.

## CONSIDERED SEISMIC INPUTS

The pounding is studied for four representative strong seismic inputs; they have been chosen according to the presence of velocity pulses and to the soil type. It has been assumed that these criteria are the most relevant to their seismic hazard. Table 3 depicts the most relevant characteristics of the considered inputs (PEER). $I_{\mathrm{A}}$ is the Arias Intensity (Arias 1970) given by $I_{\mathrm{A}} = \frac{\pi}{2\,g} \int \ddot{x}_{\mathrm{g}}^2\ dt$ where $\ddot{x}_{\mathrm{g}}$ is the input ground acceleration; the Arias intensity is an estimator of the input severity. $I_{\mathrm{D}}$ is the dimensionless seismic index (Manfredi 2001) given by $I_{\mathrm{D}} = \frac{\int \ddot{x}_{\mathrm{g}}^2\ dt}{PGA\ PGV}$. The dimensionless index accounts for the velocity pulses content; it is generally assumed that $I_D$ < 10 corresponds to impulsive registers and $I_D$ > 10 corresponds to vibratory ones. The Triffunac duration is defined as the time between the 5% and the 95% of the Arias Intensity $I_A$ (Triffunac, Brady 1975). The hypocentral distance corresponds to the straight separation between the hypocentre and the recording station. The closest distance corresponds to the shortest way to the rupture surface. $v_{s30}$ is the average shear wave velocity in the top 30 m. The soil type in the last column corresponds to the classification of the Eurocode 8 (EN-1998 2004). Table 3 shows that the Kobe input is vibratory ($I_D$ > 10) and the soil type is C, the Northridge input is impulsive ($I_D$ < 10) and the soil type is B, the Kocaeli input is impulsive ($I_D$ < 10) and the soil type is C, and the Landers input is vibratory ($I_D$ > 10) and the soil type is B.

**Table 3**. Considered input registers

| **Earthquake** | **Date** | $M_w$ | **Hypo-centre depth [km]** | **Station** | **Comp.** | **PGA [g]** | **PGV [m/s]** | $I_A$ **[m/s]** | $I_D$ | **Triffunac duration [s]** | **Hypo-central distance [km]** | **Closest distance ClsD [km]** | $V_{s30}$ **[m/s]** | **Soil type (EC8)** |
|---|---|---|---|---|---|---|---|---|---|---|---|---|---|---|
| Kobe | 16/01/1995 | 6.9 | 17.9 | Kakogawa | KAK090 | 0.345 | 0.277 | 1.687 | 11.26 | 12.86 | 30.10 | 22.5 | 312 | C |
| Northridge | 17/01/1994 | 6.7 | 17.5 | Old Ridge Route | ORR090 | 0.568 | 0.518 | 2.732 | 5.90 | 9.06 | 44.29 | 20.72 | 450.30 | B |
| Kocaeli | 17/08/1999 | 7.5 | 15 | Yarimca | YPT330 | 0.349 | 0.622 | 1.32 | 3.87 | 15.62 | 25.07 | 4.83 | 297 | C |
| Landers | 28/06/1992 | 7.3 | 7 | 24 Lucerne | LCN000 | 0.78 | 0.316 | 6.58 | 17 | 13.73 | 44.58 | 2.19 | 684.9 | B |

Figure 3 displays the time histories of the four considered ground motion records.

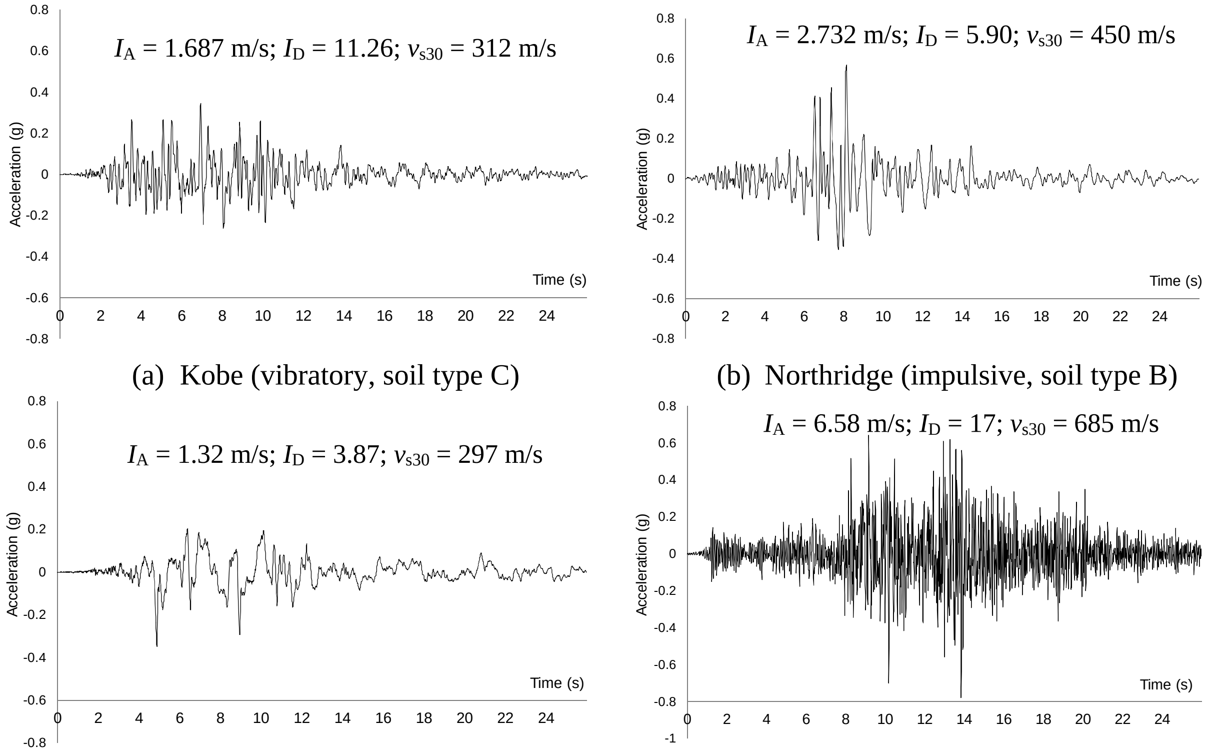


(a) Kobe (vibratory, soil type C)

(b) Northridge (impulsive, soil type B)

(c) Kocaeli (impulsive, soil type C)

(d) Landers (vibratory, soil type B)

**Figure 3**. Considered input accelerograms

## NUMERICAL RESULTS

Figure 4 through Figure 6 display preliminary results for the Northridge input (Table 3). Cases in Figure 4 through Figure 6 are described in Table 2. Figures #.a and #.b represent the maximum interstory drift displacements for the left and right building, respectively. Figures #.c and #.d show the maximum story shear force for the left and right building, respectively. Figures #.e and #.f show the hysteretic energy in each story for the left and right building, respectively. Figures #.g and #.h show the maximum absolute accelerations in the left and right building, respectively. In Figures #.a, #.b, #.c, #.d, #.g and #.h, negative and positive correspond to leftward and rightward values, respectively.

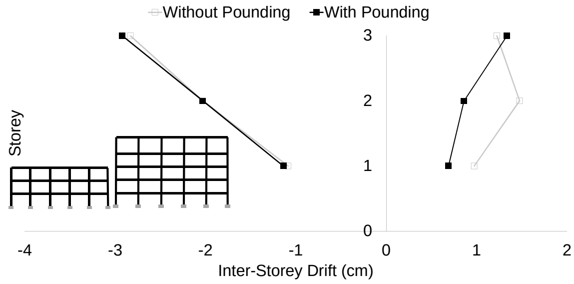


(a) Maximum inter-storey drifts in the 3×5 building

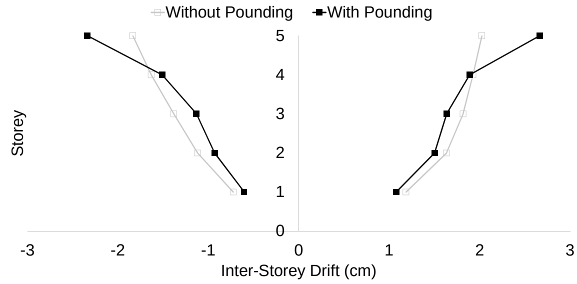


(b) Maximum inter-storey drifts in the 5×5 building

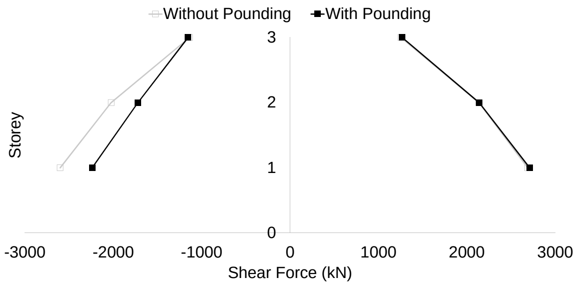


(c) Maximum storey shear force in the 3 × 5 building

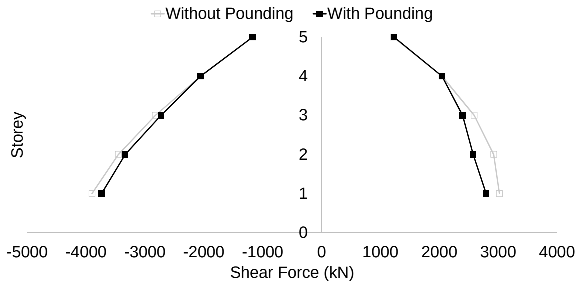


(d) Maximum storey shear force in the 5 × 5 building

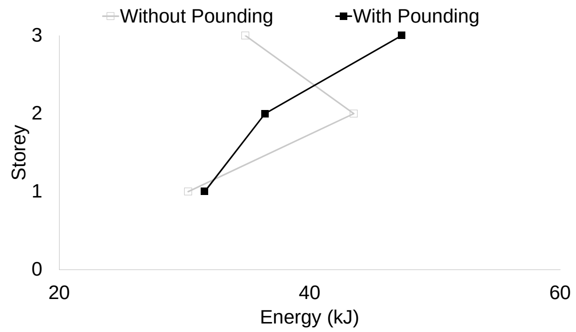


(e) Hysteretic energy in the 3 × 5 building

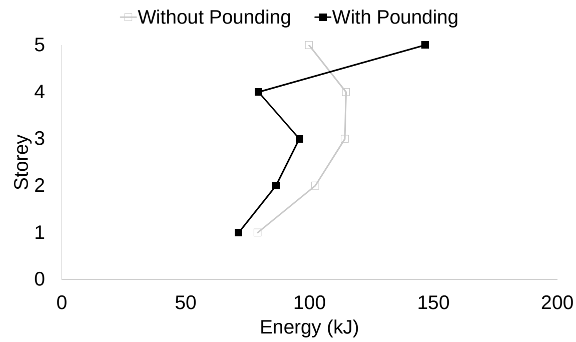


(f) Hysteretic energy in the 5 × 5 building

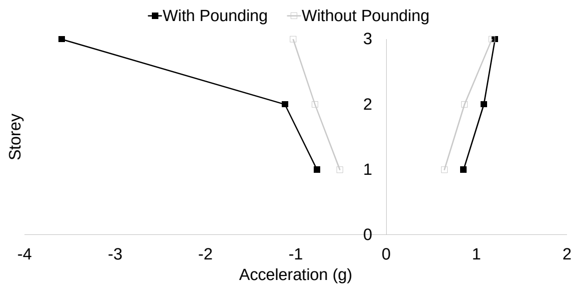


(g) Maximum absolute acceleration in the 3 × 5 building

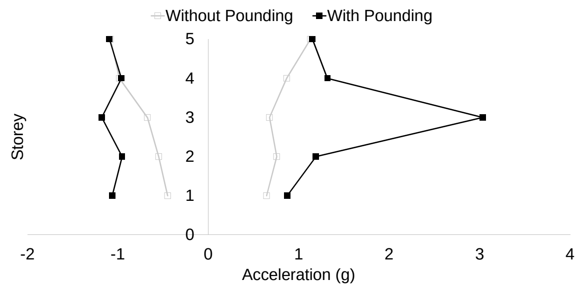


(h) Maximum absolute acceleration in the 5 × 5 building

**Figure 4**. Relevant response magnitudes. 3 × 5 | 5 × 5; $k$ = 2111 kN/mm ($\alpha$ = 5); $r$ = 0.6 ($\zeta$ = 0.16); $d$ = 2 cm. Northridge input (Table 3)

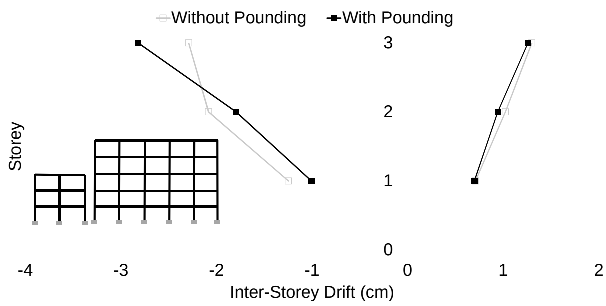


(a) Maximum inter-storey drifts in the 3×2 building

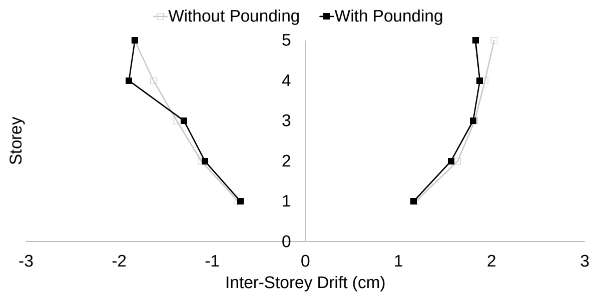


(b) Maximum inter-storey drifts in the 5 × 5 building

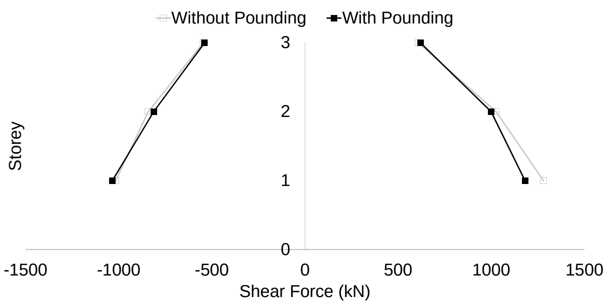


(c) Maximum storey shear force in the 3 × 2 building

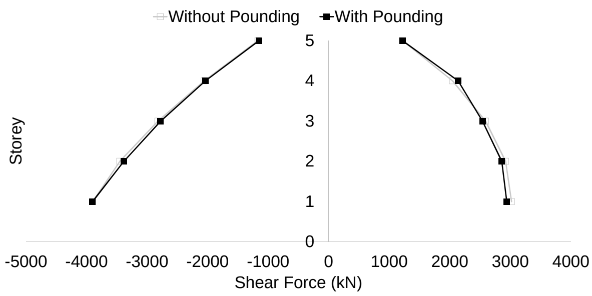


(d) Maximum storey shear force in the 5 × 5 building

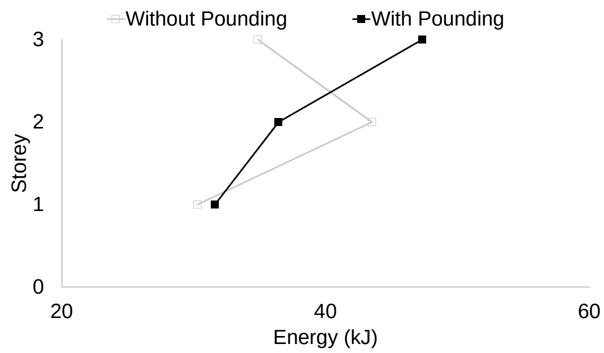


(e) Hysteretic energy in the 3 × 2 building

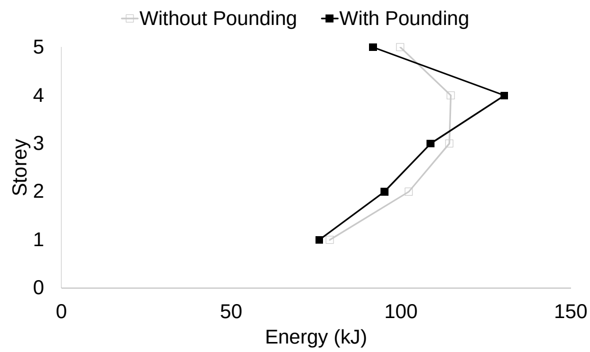


(f) Hysteretic energy in the 5 × 5 building

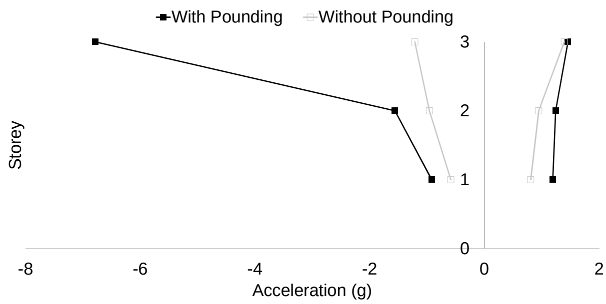


(g) Maximum absolute acceleration in the 3 × 2 building

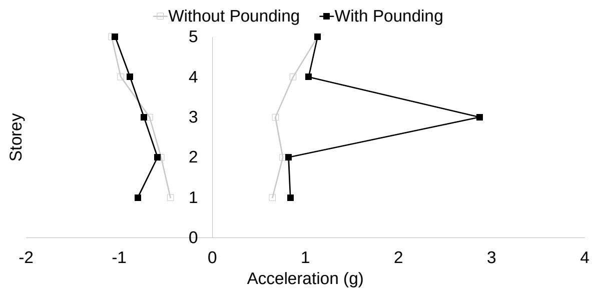


(h) Maximum absolute acceleration in the 5 × 5 building

**Figure 5**. Relevant response magnitudes. 3 × 2 | 5 × 5; $k$ = 2111 kN/mm ($\alpha$ = 5); $r$ = 0.6 ($\zeta$ = 0.16); $d$ = 2 cm. Northridge input (Table 3)

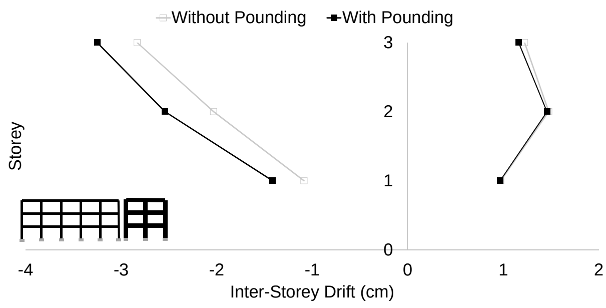


(a) Maximum inter-storey drifts in the 3×5 building

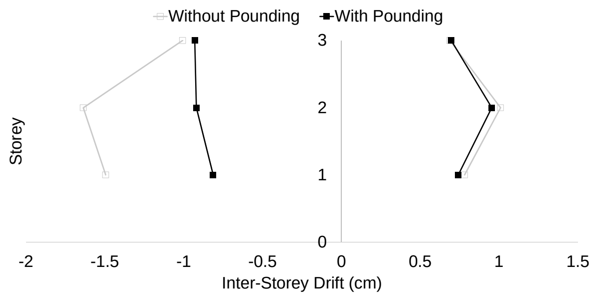


(b) Maximum inter-storey drifts in the (5 – 2) × 2 building

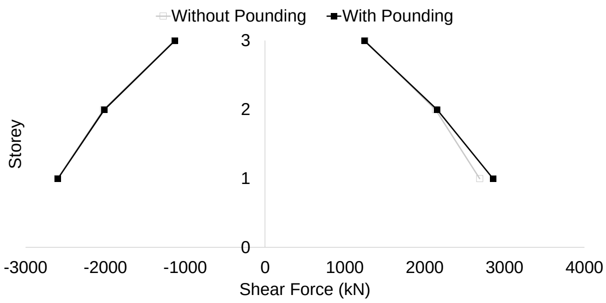


(c) Maximum storey shear force in the 3 × 5 building

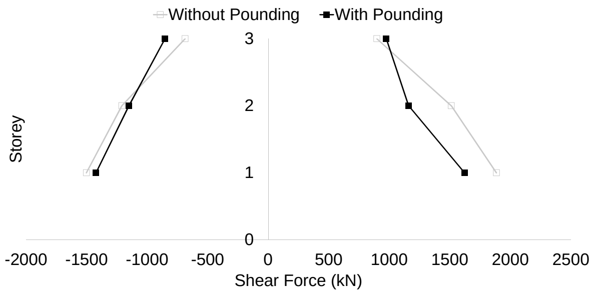


(d) Maximum storey shear force in the (5 – 2) × 2 building

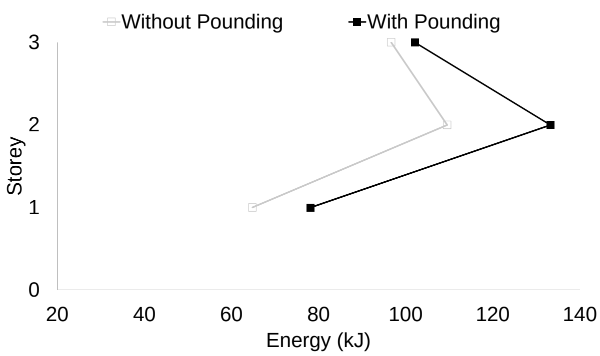


(e) Hysteretic energy in the 3 × 5 building

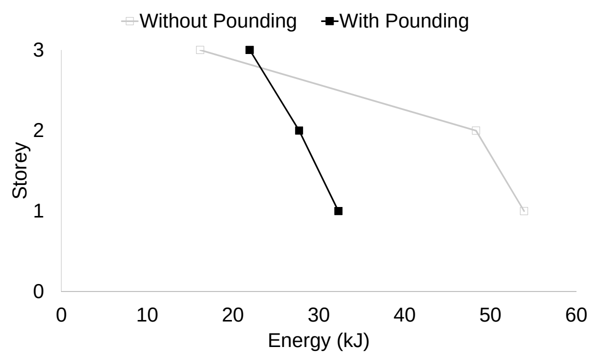


(f) Hysteretic energy in the (5 – 2) × 2 building

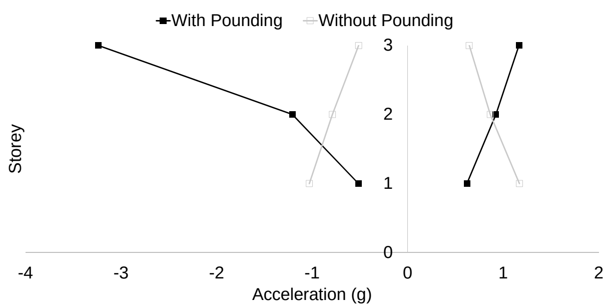


(g) Maximum absolute acceleration in the 3 × 5 building

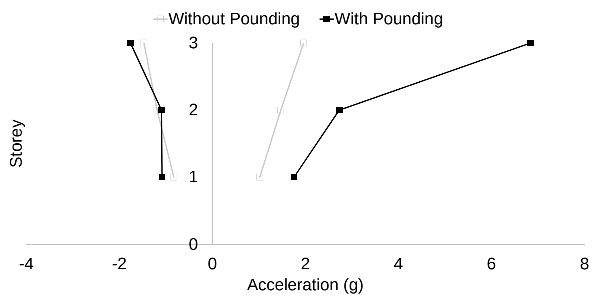


(h) Maximum absolute acceleration in the (5 – 2) × 2 building

**Figure 6**. Relevant response magnitudes. 3 × 5 | (5 – 2) × 2; $k$ = 2111 kN/mm ($\alpha$ = 5); $r$ = 0.6 ($\zeta$ = 0.16); $d$ = 2 cm. Northridge input (Table 3)

## CONCLUSIONS

This paper describes a parametrical numerical study about the consequences of pounding between adjoining short-to-mid height RC framed buildings with aligned slabs. Two 3 and 5-storey buildings designed for a high seismicity region are considered. The study consists of analysing the dynamic response of these buildings to strong seismic inputs. Pounding is described by a linear Kelvin-Voight gap model. The preliminary results in the displayed Figures show that:

- Pounding amplifies the maximum outward interstory drifts in the more flexible and less massive buildings.
- Pounding amplifies the maximum inward interstory drifts in the protruding floors (e.g., those above the top level of the shortest building) of the tallest building.
- Pounding does not affect severely the base shear and the storey shear forces.
- The behaviour of the hysteretic energy is rather similar to the one of the maximum interstory drift.
- Pounding amplifies the outward absolute accelerations in the right and left buildings, mainly in the colliding levels.

Main overall initial conclusions can be formulated as:

- The contact time is rather short.
- The pounding forces in the lowest storeys are small, being neglectable in all the cases.
- Pounding is less significant for wider gaps. In this study, if the gap is wider than 4 cm there is no pounding.
- The mass of the colliding buildings increases the effects of pounding.
- The stiffness of the gap model has a significant influence. It affects pounding forces, inter-storey drifts, absolute accelerations and base and story shear forces. This conclusion is not in complete agreement with previous studies and requires further research.
- The damping of the gap model does not have a strong influence in the pounding effects.
- The results for the four considered inputs are similar.

## REFERENCES

ACI-318-11 Building Code Requirements for Structural Concrete (2011) American Concrete Institute.

Anagnostopoulos SA (1992) “Pounding of buildings in series during earthquakes,” *Earthquake Engineering & Structural Dynamics*, 16(3): 443-456.

Anagnostopoulos SA (2004) “Equivalent viscous damping for modelling inelastic impacts in earthquake pounding problems,” *Earthquake Engineering & Structural Dynamics*, 33(8):897-902.

Arias A (1970) “A measure of earthquake intensity. Seismic Design for Nuclear Power Plants,” MIT Press 438-443.

ASCE/SEI 7-10 (2010) Minimum Design Loads for Buildings and other Structures. American Society of Civil Engineers.

Barros RC, Naderpour H, Khatami SM, Mortezaei A (2013) “Influence of Seismic Pounding on RC Buildings with and without Base Isolation System Subject to Near-Fault Ground Motions,” *Journal of Rehabilitation in Civil Engineering* 1-1 39-52.

Boyer F, Labrosse G, Chase JG, Rodgers, MacRae GA (2012) “Effects of Co-efficient of Restitution, Structural Yielding and Gap Ratios on the Impact Mechanics of Building Pounding,” *Proceedings of the 15th World Conference on Earthquake Engineering*, Lisbon (Portugal).

Chau KT, Wei XX (2001) “Pounding of structures modelled as non-linear impacts of two oscillators”, *Earthquake Engineering & Structural Dynamics*, 30:633-651.

Cole GL, Dhakal RP, Carr AJ, Bull DK (2010) “Building pounding state of the art: Identifying structures vulnerable to pounding damage,” *Proceedings of the 2010 NZSEE Conference*, Wellington, New Zealand, March 26-28, 2010.

Dimitrakopoulos E, Kappos AJ, Makris N (2009a) “Dimensional analysis of the earthquake-induced pounding between adjacent structures”*Earthquake Engineering & Structural Dynamics* 38:867–886.

Dimitrakopoulos E, Kappos AJ, Makris N (2009b) “Dimensional analysis of yielding and pounding structures for records without distinct pulses” *Soil Dynamics & Earthquake Engineering* 29 1170–1180.
Efraimiadou S, Hatzigeorgiou GD, Beskos DE (2013) “Structural pounding between adjacent buildings subjected to strong ground motions. Part I: The effect of different structures arrangement”, *Earthquake Engineering & Structural Dynamics*, 42:1509–1528.
EN-1998. Eurocode 8: Design of structures for earthquake resistance (2004) European Committee for Standardization.
Favvata MJ, Karayannis CG, Anagnostopoulou V (2012) “Influence of infill panels with and without openings on the pounding effect of RC structures,” *Proceedings of the 15th World Conference on Earthquake Engineering*, Lisbon (Portugal).
Jankowski R (2005) “Non-linear viscoelastic modelling of earthquake-induced structural pounding,” *Earthquake Engineering & Structural Dynamics*, 34:595–611.
Jankowski R (2006a) “Pounding force response spectrum under earthquake excitation,” *Engineering Structures*, 28 (2006) 1149–1161.
Jankowski R (2006b) “Analytical expression between the impact-damping ratio and the coefficient of restitution in the nonlinear viscoelastic model of structural pounding,” *Earthquake Engineering & Structural Dynamics*, 35:175–524.
Jankowski R (2008) “Earthquake-induced pounding between equal height buildings with substantially different dynamic properties,” *Engineering Structures*, 30:2818–2829.
Jankowski R (2010) “Experimental study on earthquake-induced pounding between structural elements made of different building materials,” *Earthquake Engineering & Structural Dynamics*, 39:343–354.
Karayannis CG, Favvata MJ (2005) “Earthquake-induced interaction between adjacent reinforced concrete structures with non-equal heights,” *Earthquake Engineering & Structural Dynamics*, 34:1–20.
Khatiwada S, Chouw N, Butterworth JW (2014) “A generic structural pounding model using numerically exact displacement proportional damping,” *Engineering Structures*, 62-63:33-41.
Madas P (1993) “Advanced Modelling of Composite Frames Subjected to Earthquake Loading,” *PhD Thesis*, Imperial College, London, UK.
Maison BF, Kasai K (1992) “Dynamics of pounding when two buildings collide,” *Earthquake Engineering & Structural Dynamics,* 21(9):771–786.
Mander JB, Priestley MJN, Park R (1988) “Theoretical stress-strain model for confined concrete,” *Journal of Structural Engineering*, 114(8):1804-1826.
Manfredi G (2001) “Evaluation of Seismic Energy Demand,” *Earthquake Engineering & Structural Dynamics*, 30:485–499.
Martínez-Rueda JE, Elnashai AS (1997) “Confined concrete model under cyclic load,” *Materials and Structures*, 30(197):139-147.
Muthukumar S, DesRoches R (2006) “A Hertz contact model with non-linear damping for pounding simulation,” *Earthquake Engineering & Structural Dynamics*, 35:811–828.
Pantelides CP, Ma X (1998) “Linear and nonlinear pounding of structural systems”, Computers & Structures Vol. 66. No. 1, 79-92.
Papadrakakis M, Apostolopoulou C, Zacharopoulos A, T Bitzarakis S (1996) “Three-dimensional simulation of structural pounding during earthquakes”, *Journal of Engineering Mechanics* 122:423-431.
PEER Ground Motion Database. http://peer.berkeley.edu/products/strong_ground_motion_db.html.
Raj Pant D, Wijeyewickrema AC, Ohmachi T (2010) “Seismic Pounding between Reinforced Concrete Buildings: A Study using two recently proposed Contact Element Models”, *Proceedings of the 14th European Conference on Earthquake Engineering*, Ohrid (Macedonia).
Ruangrassamee A, Kawashima K (2001) “Relative displacement response spectra with pounding effect”, *Earthquake Engineering & Structural Dynamics*, 30:1511–1538.
Seismosoft (2013) “SeismoStruct v6.5 – A computer program for static and dynamic nonlinear analysis of framed structures,” available from http://www.seismosoft.com.
Triffunac MD, Brady AG (1975) “Study on the duration of strong earthquake ground motion,” *Bulletin of the Seismological Society of America* 65(3):581–626.
Yaghmaei-Sabegh S, Jalali-Milani N (2012) “Pounding force response spectrum for near-field and far-field earthquakes,” *Scientia Iranica Transactions A: Civil Engineering* 19(5):1236–1250.
Ye K, Li L, Zhu H (2009) “A note on the Hertz contact model with nonlinear damping for pounding simulation,” *Earthquake Engineering & Structural Dynamics*, 38:1135–1142.